

AdS plane waves and entanglement entropy

K. Narayan, Tadashi Takayanagi and Sandip P. Trivedi

^a*Chennai Mathematical Institute,
SIPCOT IT Park, Siruseri 603103, India.*

^b*Yukawa Institute for Theoretical Physics, Kyoto University,
Kitashirakawa Oiwakecho, Sakyo-ku, Kyoto 606-8502, Japan.*

^c*Department of Theoretical Physics, Tata Institute of Fundamental Research,
Homi Bhabha Road, Colaba, Mumbai 400005, India.*

Abstract

AdS plane waves describe simple backgrounds which are dual to anisotropically excited systems with energy fluxes. Upon dimensional reduction, they reduce to hyperscaling violating spacetimes: in particular, the AdS_5 plane wave is known to exhibit logarithmic behavior of the entanglement entropy. In this paper, we carry out an extensive study of the holographic entanglement entropy for strip-shaped subsystems in AdS plane wave backgrounds. We find that the results depend crucially on whether the strip is parallel or orthogonal to the energy current. In the latter case, we show that there is a phenomenon analogous to a phase transition.

1 Introduction

The entanglement entropy is a very useful quantity which characterizes the ground state of a quantum many-body system. It can be used as a quantum order parameter to distinguish various quantum phases. Recently, entanglement entropy has been actively explored both from the string theory side and the condensed matter theory side. For example, the properties of entanglement entropy of ground states have been studied from the field theoretic approach [1] and the holographic approach [2]. However, our understanding of quantum entanglement of excited states in quantum many-body systems is still limited at present.

It is well-known that the entanglement entropy correctly measures the amount of quantum entanglement only for pure states. On the other hand, if we compute the entanglement entropy for a finite temperature system as an example of mixed state, it includes a contribution from the thermal entropy in addition to that from the quantum entanglement. Therefore we need to look at pure excited states in order to estimate the quantum entanglement by employing the entanglement entropy. One such example is an excited state created by a quantum quench, which is typically induced by a sudden shift of parameters in a given quantum system. The entanglement entropy increases under time evolution after the quantum quench. In two dimensional conformal field theories (CFTs), some analytical results have been known [3]. Holographic calculations have been done for any dimension [4, 5]. In these examples, the systems are excited homogeneously and isotropically. Since the holographic description of quantum quenches requires complicated numerical calculations of black hole formation in general, it is quite difficult to get analytical results on the behavior of entanglement entropy¹.

The purpose of this paper is to study entanglement entropy in a more tractable setup. Specifically we consider a CFT with a constant energy flux T_{++} . This offers us a simple model of anisotropically excited states with energy flow. It is holographically dual to an AdS space with a plane wave [7, 8, 9] (similar solutions in the form of shock waves in *AdS* have been studied previously *e.g.* [10, 11, 12]). To define the entanglement entropy we need to specify a subsystem which we trace out. We choose the subsystem to be a strip with a finite width. Interestingly we will find that the behavior of the holographic entanglement entropy (HEE) crucially depends on the direction of the strip.

After a light-like compactification, as shown in [7, 8, 9], these AdS plane wave backgrounds become gravity duals with hyperscaling violation: the AdS_5 plane wave in particular gives a space-time exhibiting logarithmic behavior of entanglement entropy. Such a background can be realized

¹Nevertheless, a universal relation which is analogous to thermodynamics has been found recently in [6] for a small size subsystem.

in effective Einstein-Maxwell-Dilaton theories [13, 14, 15, 16, 17, 18, 19, 20, 21, 22] and has been expected to be dual to non-Fermi liquids [23, 24] (see also [25, 7, 26, 8, 27, 28, 29, 30, 9] for string realizations and further discussion).

The paper is organized as follows. In section 2, we review *AdS* plane wave backgrounds. In section 3, we present results of holographic calculations of entanglement entropy in the *AdS* plane wave for the case where the strip subsystem is parallel with the energy current. In section 3, we study the holographic entanglement entropy when the subsystem is orthogonal to the energy current and show that there is a behavior analogous to a phase transition. In section 5, we summarize our conclusions.

2 Reviewing AdS Plane Waves

The gravity/5-form sector of IIB string theory contains the *AdS*₅ plane wave [7] (see also [8, 9])

$$ds^2 = \frac{R^2}{r^2} [-2dx^+ dx^- + \sum_{i=1}^2 dx_i^2 + dr^2] + R^2 Q r^2 (dx^+)^2 + R^2 d\Omega_5^2, \quad R^4 \sim g_{YM}^2 N \alpha'^2, \quad (1)$$

as a solution with no other sources, with Q a parameter of dimension (boundary) energy density, and $d\Omega_5^2$ being the metric on S^5 (or other Einstein space). Equivalently, the 5-dim part of the metric is a solution to $R_{MN} = -\frac{4}{R^2} g_{MN}$ arising in the effective 5-dim gravity system with negative cosmological constant: the g_{++} deformation is a normalizable one. From the holographic stress tensor calculation, one obtains

$$T_{++} = \frac{Q}{4\pi G_5}. \quad (2)$$

Thus we see that this spacetime is dual to an excited state in the boundary $\mathcal{N}=4$ SYM conformal field theory with uniform constant lightcone momentum density turned on. These spacetimes correspond to a (chiral) wave on the boundary. Imposing a null energy condition, we have $T_{++} \sim Q \geq 0$.

This spacetime (1) can be obtained [8] as a “zero temperature” double-scaling limit of boosted black D3-branes, using *e.g.* [31]: to elaborate, consider black D3-branes (*i.e.* *AdS*₅ Schwarzschild spacetimes) with metric $ds^2 = r^2 [-(1 - r_0^4 r^4) dt^2 + dx_3^2 + \sum_{i=1}^2 dx_i^2] + \frac{dr^2}{r^2(1 - r_0^4 r^4)}$ and define $t = \frac{x^+ + x^-}{\sqrt{2}}$, $x_3 = \frac{x^+ - x^-}{\sqrt{2}}$, with lightcone coordinates x^\pm : after boosting by λ as $x^\pm \rightarrow \lambda^{\pm 1} x^\pm$, we obtain

$$ds^2 = \frac{1}{r^2} \left[-2dx^+ dx^- + \frac{r_0^4 r^4}{2} (\lambda dx^+ + \lambda^{-1} dx^-)^2 + \sum_{i=1}^2 dx_i^2 \right] + \frac{dr^2}{r^2(1 - r_0^4 r^4)}. \quad (3)$$

Note that we have set the *AdS* radius R to unity here. Now in the double scaling limit $r_0 \rightarrow 0$, $\lambda \rightarrow \infty$, with $Q = \frac{r_0^4 \lambda^2}{2}$ fixed, (3) reduces to (1). (For $r_0 = 0$, this is just *AdS*₅ in lightcone coordinates.)

Rewriting this in terms of just Q, r_0 , gives

$$ds^2 = \frac{1}{r^2} \left[-2dx^+ dx^- + Qr^4 (dx^+ + \frac{r_0^4}{2Q} dx^-)^2 + \sum_{i=1}^2 dx_i^2 \right] + \frac{dr^2}{r^2(1 - r_0^4 r^4)}. \quad (4)$$

From [31], we see that we now have other energy-momentum components also turned on,

$$T_{++} \sim \lambda^2 r_0^4 \sim Q, \quad T_{--} \sim \frac{r_0^4}{\lambda^2} \sim \frac{r_0^8}{Q}, \quad T_{+-} \sim r_0^4, \quad T_{ij} \sim r_0^4 \delta_{ij}. \quad (5)$$

Turning on a small r_0 about (1), this means T_{++} is dominant while the other components are small. In some sense, this is like a large left-moving chiral wave with $T_{++} \sim Q$, with a small amount of right-moving stuff turned on. This spacetime interpolates between the usual unboosted black D3-brane ($\lambda = 1$, *i.e.* $Q = \frac{r_0^4}{2}$) and the AdS_5 plane wave ($\lambda \rightarrow \infty$, with Q fixed). There are two nontrivial scales here, Q and r_0 : for small r_0 , we expect that physical observables such as entanglement entropy are dominated by the AdS plane wave limit, *i.e.* by Q , with small r_0 -dependent corrections.

Let us now consider x^+ -dimensional reduction of (1) as in [7]: the 5-dim part of this metric can be rewritten (relabelling $x^- \equiv t$) as, $ds^2 = R^2(-\frac{dt^2}{Qr^6} + \frac{\sum_{i=1}^2 dx_i^2 + dr^2}{r^2} + Qr^2(dx^+ - \frac{dt}{Qr^4})^2)$. This gives the effective (bulk) 3 + 1-dim Einstein metric and exponents

$$ds_E^2 = \frac{R^3 \sqrt{Q}}{r} \left(-\frac{dt^2}{Qr^4} + \sum_{i=1}^2 dx_i^2 + dr^2 \right), \quad \theta = 1, \quad z = 3, \quad (6)$$

along with an electric gauge field $A = -\frac{dt}{Qr^4}$ and scalar $e^\phi \sim r$. Above, we have compared with the hyperscaling violating metric in the form $ds^2 = r^{2\theta/d_i}(-\frac{dt^2}{r^{2z}} + \frac{\sum_{i=1}^2 dx_i^2 + dr^2}{r^2})$, with boundary spatial dimension d_i . This lies in the hyperscaling violating family “ $\theta = d_i - 1$ ” exhibiting logarithmic behavior of entanglement entropy (as we will review later) and has thus been argued to correspond to a gravitational dual description of a theory with hidden Fermi surfaces [23, 24](see also [25]). It is thus interesting to explore these AdS plane waves further, in particular from the higher dimensional point of view.

More generally, we have the (purely gravitational) AdS_{d+1} deformation, which is the AdS_{d+1} plane wave,

$$ds^2 = \frac{R^2}{r^2} \left(-2dx^+ dx^- + \sum_{i=1}^{d-2} dx_i^2 + dr^2 \right) + R^2 Q r^{d-2} (dx^+)^2, \quad (7)$$

the x_i being $(d-1)$ -dim (boundary) spatial coordinates, with Q a parameter of energy density in d -dimensions. This is a solution to $R_{MN} = -\frac{d}{R^2} g_{MN}$, *i.e.* to gravity with a negative cosmological constant. It is also useful to introduce the time and space coordinate (t, x_{d-1}) such that

$$x^\pm = \frac{t \pm x_{d-1}}{\sqrt{2}}. \quad (8)$$

This can then be used to obtain the spacetime (7) as a double-scaling limit of the AdS_{d+1} black brane in lightcone coordinates near a double-scaling limit [8], resulting in a near-extremal AdS_{d+1} plane wave: most of our discussion with the regulated (finite temperature) case will be for the AdS_5 plane wave.

Now, dimensionally reducing on the x^+ -dimension (and relabelling $x^- \equiv t$) gives the metric and exponents

$$ds_E^2 = \frac{R^2(R^2Q)^{1/(d-2)}}{r} \left(-\frac{dt^2}{Qr^d} + \sum_{i=1}^{d-2} dx_i^2 + dr^2 \right), \quad z = \frac{d-2}{2} + 2, \quad \theta = \frac{d-2}{2}. \quad (9)$$

For the special case of $d-2=2$, this θ value lies in the special family “ $\theta = d_i - 1$ ” as we have seen above². From the lower dimensional point of view (the “#” are numerical constants), the d -dim action $\int d^{d+1}x \sqrt{-g^{(d+1)}} (R^{(d+1)} - 2\Lambda)$ dimensionally reduces as

$$\int dx^+ d^d x \sqrt{-g^{(d)}} (R^{(d)} - \# \Lambda e^{-2\phi/(d-2)} - \#(\partial\phi)^2 - \#e^{2(d-1)\phi/(d-2)} F_{\mu\nu}^2), \quad (10)$$

where the scalar is $g_{d+1,d+1} = e^{2\phi}$, the (purely electric) gauge field is $A = -\frac{dt}{r^d}$ and the d -dimensional metric undergoes a Weyl transformation as $g_{\mu\nu}^{(d)} = e^{2\phi/(d-2)} g_{\mu\nu}^{(d+1)}$. It is straightforward to check that the solution (9) is consistent with the equations of motion, with the scalar of the form $e^{2\phi} = r^{d-2}$.

There is a more general family of AdS null deformations [9] which include inhomogenous AdS plane waves, of the form $ds^2 = \frac{1}{r^2}[-2dx^+ dx^- + \sum_{i=1}^2 dx_i^2 + dr^2] + g_{++}(dx^+)^2 + d\Omega_5^2$, with $g_{++}(r, x_i)$ spatially varying. This also includes the case $g_{++} \xrightarrow{r \rightarrow 0} const = K$, sourced by other matter fields, which are asymptotic to $z=2$ 4-dim Lifshitz spacetimes upon x^+ -dimensional reduction [32]. All these solutions, including (1), have finite curvature invariants everywhere, which are the same as those for $AdS_5 \times S^5$. Furthermore, they all preserve some supersymmetry. Due to the lightlike nature, nonzero contractions involving curvature components vanish (this can be checked explicitly for low orders) and thus these spacetimes are likely to be α' -exact, somewhat analogous to plane waves and $AdS_5 \times S^5$. This makes them possibly more interesting as string backgrounds.

It is worth noting the possibility of tidal forces diverging in the deep interior $r \rightarrow \infty$, even though curvature invariants are regular and the same as in $AdS_5 \times S^5$: this is a general feature of plane wave (and in fact any lightlike) spacetimes. This may reflect the fact that from the lower dimensional point of view, we have a hyperscaling violating spacetime, which is conformal to Lifshitz, and there are curvature singularities arising from the conformal factor (unlike Lifshitz spacetimes which only have diverging tidal forces); see *e.g.* [33] for a recent discussion. From the field theory point of view, this is the question of whether turning on uniform T_{++} density has

²Note that the d_i in the expression $\theta = d_i - 1$ is the boundary spatial dimension, while we are discussing AdS_{d+1} plane waves with d the boundary spacetime dimension in the higher dimensional description.

certain pathologies. From the bulk point of view, this sort of a singularity if it exists is often regarded as mild, possibly regulated by finite temperature effects. In this sense, thinking of the homogenous AdS plane wave as a zero temperature “chiral” limit of the boosted black brane is useful: physically any singularity will be cloaked by the finite temperature horizon. From the dual point of view, we are considering a certain boosted limit of thermal states in the CFT: for finite (if large) boost, we expect this is well-behaved.

2.1 Entanglement Entropy for Light-like Subsystems in AdS_5 Plane Wave

The entanglement entropy S_A for the subsystem A is defined by $S_A = -\text{tr}\rho_A \log \rho_A$, where ρ_A is defined by tracing out the density matrix ρ for the total system over the subsystem B , which is the complement of A , i.e. $\rho_A = \text{tr}_B \rho$. In any backgrounds of AdS/CFT, we can holographically calculate the entanglement entropy S_A from the area of extremal surface γ_A which ends on the boundary of A . An extremal surface is defined by the one whose area functional gets stationary under any infinitesimal deformations with a fixed boundary condition. The area is calculated in terms of the Einstein frame. If there are several extremal surfaces, we need to pick up the one with the minimal area among them. This is called the (covariant) holographic entanglement entropy (HEE) [4]:

$$S_A = \text{Min}_{\gamma_A \in ES.} \left[\frac{\text{Area}(\gamma_A)}{4G_N^{(d+1)}} \right], \quad (11)$$

where $G_N^{(d+1)}$ is the Newton constant in the $d+1$ dimensional gravity theory we consider. In static backgrounds, since we can restrict to a time slice, γ_A is reduced to a minimal area surface on that slice and leads to the minimal surface prescription [34]. In many parts of this paper we will omit the factor $\frac{1}{4G_N^{(d+1)}}$ because we are mainly interested in the dependence on the size of the subsystem and thus the overall factor is not important for our purpose.

We now review the logarithmic violation of the area law for entanglement entropy in the AdS_5 plane wave, using the HEE (11) and finding the area of a bulk minimal surface bounding a subsystem A in the shape of a strip in the x_1, x_2 -plane. From the point of view of the lower dimensional theory obtained by x^+ -dimensional reduction, it is natural to consider subsystems A that extend along the x^+ -direction completely, and the corresponding bulk minimal surface lying on a constant lightcone time x^- slice (which corresponds to a constant time slice since $x^- \equiv t$).

Consider a strip region in the x_1 -direction given by $-l \leq x_1 \leq l$, extending along the x_2 -direction: the minimal surface is parametrized by $x = x(r)$, and its area gives the entanglement entropy

$$S_A = \frac{1}{2G_N^{(5)}} \int_0^L \frac{R dy}{r} \int_0^{L^+} \sqrt{g_{++}} dx^+ \int \frac{R \sqrt{dx^2 + dr^2}}{r} = \frac{LL_+ R^3 \sqrt{Q}}{2G_N^{(5)}} \int_\epsilon^{r^*} dr \frac{\sqrt{1 + (x')^2}}{r}, \quad (12)$$

where ϵ is the near-boundary cutoff (*i.e.* the UV cutoff in the field theory). The minimal surface has a turning point r_* where $\frac{dr}{dx}|_{r_*} = 0$. The minimal surface then is given by the half circle:

$$x = \sqrt{l^2 - r^2}, \quad (13)$$

and thus we can estimate as

$$S_A = \frac{L_+ R^3 \sqrt{Q}}{2G_N^{(5)}} L \log \frac{l}{\epsilon}. \quad (14)$$

Using $G_N^{(4)} = \frac{G_N^{(5)}}{L_+}$, this gives the logarithmic behavior, as expected from the lower dimensional theory. We have effectively taken $l \gg \epsilon$, so that the strip width l is macroscopic relative to the UV cutoff ϵ in the field theory. When the strip size shrinks to roughly the cutoff, we have a cross-over to the UV behaviour in the field theory: in this case, we expect the entanglement entropy for AdS_5 in lightcone time slicing which vanishes, as vindicated by (14) for $l \sim \epsilon$. As $Q \rightarrow 0$, this surface degenerates and becomes null, and the corresponding area vanishes.

Note that this calculation (14) above arises from just the 5-dim part of the spacetime, so it also applies to $AdS_5 \times X^5$ plane waves dual to various $\mathcal{N}=1$ super Yang-Mills theories.

3 Entanglement Entropy in AdS Plane Wave: Case A

The purpose of this paper is to give an extensive study of holographic entanglement entropy in the AdS plane wave background (7) and its regularized one. Especially we will look at the entanglement entropy S_A when the subsystem A is given by a (infinitely extended) strip with a finite width l at a constant time. Then the entanglement entropy consists of two terms: one is the area law divergence [35] and the other is the finite term [36, 34]. We expect that the area law divergence remains the same as that for the pure AdS dual to the ground state, while the subleading finite term will be modified in our excited backgrounds.

There are two different choices of such systems depending on whether the finite width direction is (a) either of $(x_1, x_2, \dots, x_{d-2})$, called case A or (b) x_{d-1} , called case B (see Fig.1). We will study the case A below and the case B in the next section because in the latter case, a more careful analysis is needed. Notice that in case A, the energy current is parallel with the strip, while it is orthogonal in case B.

3.1 Holographic Analysis in Case A

In case A, the width direction is orthogonal to x_+ and x_- . We can take it to be along x_1 . Thus we need to assume $d \geq 3$. Then the subsystem A is specified by

$$0 \leq x_1 \leq l, \quad (x_+, x_-) = (\alpha y, -\beta y), \quad -\infty < y, x_2, x_3, \dots, x_{d-2} < \infty. \quad (15)$$

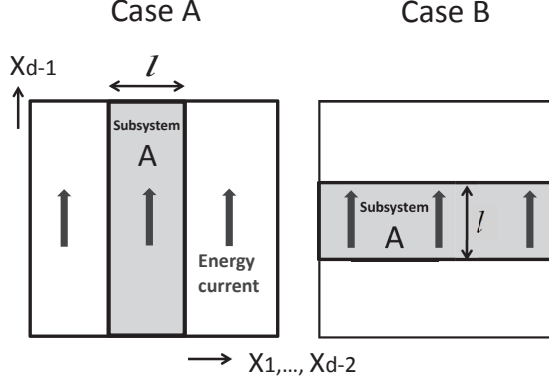


Figure 1: The two different choices of the strip subsystem A . The gray arrows represents the energy current. The left and right are called case A and case B, respectively.

The extremal surface γ_A is specified by the function $x_1 = x(r)$. We define the maximal value of r to be r_* , where γ_A turns around, changing the sign of $\frac{dr}{dx}$.

The area functional is given by

$$\text{Area} = R^{d-1} V_{d-2} \cdot 2\sqrt{\alpha} \int_{\epsilon}^{r_*} dr r^{-(d-1)} \sqrt{(1+x'^2)(2\beta + Qr^d\alpha)}, \quad (16)$$

where V_{d-2} denotes the (infinite) volume in the y and (x_2, \dots, x_{d-2}) direction. The infinitesimally small parameter ϵ represents the UV cut off.

The extremal surface is specified by the function $x_1 = x(r)$. The equation of motion leads to

$$\partial_r x = \frac{Ar^{d-1}}{\sqrt{2\beta + Q\alpha r^d - A^2 r^{2(d-1)}}}, \quad (17)$$

where A is the integration constant. Note that at $r = r_*$, the denominator of the right hand side of (17) vanishes. Thus we find

$$l = 2 \int_0^{r_*} dr \frac{Ar^{d-1}}{\sqrt{2\beta + Q\alpha r^d - A^2 r^{2(d-1)}}}. \quad (18)$$

Now the area functional is rewritten as

$$\text{Area} = 2\sqrt{\alpha} V_{d-2} R^{d-1} \int_{\epsilon}^{r_*} \frac{dr}{r^{d-1}} \cdot \frac{2\beta + Q\alpha r^d}{\sqrt{2\beta + Q\alpha r^d - A^2 r^{2(d-1)}}}. \quad (19)$$

3.2 Behavior of Entanglement Entropy

The entanglement entropy S_A in a quantum field theory is defined for a subsystem A which is on a constant time slice. This corresponds to the choice $\beta = \alpha = 1$. In this case, the leading divergence

is the standard area law

$$S_A \sim O(\epsilon^{-(d-2)}). \quad (20)$$

The effects due to non-vanishing flux Q turn out to be finite. When Q and l are both large, we find $l \sim r_*$ and $Qr_*^d \simeq A^2 r_*^{2(d-1)} \gg 1$. In this case, we find that the finite part of S_A behaves like³

$$S_A|_{finite} \sim \pm V_{d-2} \sqrt{Q} \cdot l^{2-\frac{d}{2}}. \quad (21)$$

The sign in front of (21) is + for $d < 4$ and - for $d > 4$. In the case $d = 4$ we need to replace (21) with

$$S_A|_{finite} \sim V_2 \sqrt{Q} \cdot \log \left(l \cdot Q^{\frac{1}{4}} \right). \quad (22)$$

In general, when l is large, the above result is smaller than that of the thermal entropy, which is extensive and is proportional to l , while it is larger than the finite contribution in CFTs at zero temperature, which scales like $\sim O(l^{-(d-2)})$. Moreover, the finite contribution is a monotonically increasing function of l . This agrees with our intuitive expectation: the active degrees of freedom should increase because the energy flow excites the system.

We can also consider disconnected extremal surfaces defined by $x(r) = \text{const.}$, which extend from $r = \epsilon$ to the deep IR limit $r = \infty$. However, they always give larger areas and therefore do not contribute. When $d \leq 4$, it is clear that the IR contributions to the areas diverge as $\int_{\epsilon}^{\infty} dr r^{1-d/2} = \infty$. When $d > 4$, their contributions are finite, but numerically we could confirm that they are larger than the connected area (19). This situation is similar to the holographic calculations in the pure AdS spaces.

Two more comments are worth making. First, when $d = 3$, so that one is dealing with the AdS_4 plane wave and a 2 + 1 dimensional boundary theory, the finite part of S_A in eq.(21) becomes

$$S_A|_{finite} \sim V_1 \sqrt{Q} \sqrt{l} \quad (23)$$

where V_1 is the length of the region in the y direction. We see that the log term in $d = 4$ is replaced by a power law enhancement going like \sqrt{l} . While examples of string constructions or constructions in gauged supergravity giving rise to hyperscaling violating geometries are well known, to our knowledge, the AdS plane wave is the first example of a string construction which gives rise to such a power law enhancement.

Second, note that the AdS plane wave solution represents a valid state in any CFT which admits a smooth gravity dual since it arises simply from the AdS Schwarzschild solution in the limit of infinite boost. As such, our result for the entanglement entropy in eq.(21) is also quite

³Here we omitted factors like $\frac{1}{G_N^{(d+1)}}$ as we are not interested in the overall factor which is fixed once the CFT is given.

general applying, for example in the $d = 4$ case to the $\mathcal{N}=4$ SYM theory, the Klebanov-Witten theory from D3-branes on the conifold, and more general $\mathcal{N}=1$ superconformal Yang-Mills theories dual to $AdS_5 \times X^5$ (where X^5 is the Sasaki-Einstein base space of the Calabi-Yau cone where the D3-branes are stacked), and in the $d = 3$ case to the M2 brane theory, ABJM theory etc.

3.3 Light-like Limit

The limit where A gets light-like is given by $\beta = 0$. This corresponds to a generalization of entanglement entropy and its precise definition in quantum field theory can be given by the replica method at least formally (analogous to [3]).

We can also set $\alpha = 1$ without losing generality. Then we find $l \sim r_*$. Thus it is clear that the leading term with respect to $\epsilon (\rightarrow 0)$ behaves

$$S_A \sim V_{d-2} \sqrt{Q} \cdot O(\epsilon^{2-\frac{d}{2}}). \quad (24)$$

Thus, S_A is finite for $d < 4$. For $d = 4$, S_A is logarithmically divergent [7]

$$S_A \sim V_2 \sqrt{Q} \cdot \log \frac{l}{\epsilon}, \quad (25)$$

as we reviewed in subsection 2.1. Note that the divergence is always smaller than the space-like case $\beta \neq 0$.

3.4 Analysis in Regularized AdS Plane Wave

The above calculations can be repeated for the regulated or near-extremal AdS_5 plane wave (4), with finite boost λ . We obtain

$$S_A \sim V_2 \int \frac{dr}{r^3} \sqrt{(\partial_r x)^2 + \frac{1}{1-r_0^4 r^4}} \sqrt{2\alpha\beta + Qr^4 \left(\alpha - \frac{\beta r_0^4}{2Q}\right)^2} \quad (26)$$

giving

$$\partial_r x = \frac{1}{1-r_0^4 r^4} \frac{pr^3}{\sqrt{2\alpha\beta + Qr^4 \left(\alpha - \frac{\beta r_0^4}{2Q}\right)^2 - p^2 r^6}}, \quad (27)$$

and thus

$$S_A \sim V_2 \int \frac{dr}{r^3} \frac{2\alpha\beta + Qr^4 \left(\alpha - \frac{\beta r_0^4}{2Q}\right)^2}{\sqrt{1-r_0^4 r^4} \sqrt{2\alpha\beta + Qr^4 \left(\alpha - \frac{\beta r_0^4}{2Q}\right)^2 - p^2 r^6}}. \quad (28)$$

For $\beta = 0$, we have a lightlike surface, giving $S_A \sim V_2 \sqrt{Q} \int \frac{dr}{r} \frac{1}{\sqrt{(1-\frac{p^2 r^2}{Q\alpha^2})(1-r_0^4 r^4)}}$ with a logarithmic

leading divergence as before. In addition we have a finite subleading piece $V_2 \sqrt{Q} \frac{r_0^4}{l^4}$ which is cutoff independent. For large size, we expect that the surface wraps part of the horizon.

For a spacelike surface, we can take $\alpha = \beta = 1$ as before, and the leading divergence reflects the area law. Taking r_0 small, we expect the extremal surface to be essentially governed by the AdS plane wave background, with corresponding entanglement entropy.

As a check, note that in the limit where $Q = \frac{r_0^4}{2}$ *i.e.* the familiar black D3-brane, taking $\alpha = \beta = 1$, we recover the familiar expression $S_A \sim V_2 \int \frac{dr}{r^3} \frac{2}{\sqrt{1-r_0^4 r^4} \sqrt{2-p^2 r^6}}$ for the black D3-brane.

4 Entanglement Entropy in AdS Plane Wave: Case B

Next we study the case B where the width direction of the strip A is parallel to x_{d-1} . More generally we assume that the strip A is defined by

$$-\frac{\Delta x^+}{2} \leq x^+ \leq \frac{\Delta x^+}{2}, \quad -\frac{\Delta x^-}{2} \leq x^- \leq \frac{\Delta x^-}{2}, \quad -\infty < x_i < \infty. \quad (29)$$

We will denote the regularized length in each of the x_i directions by $L(\gg l)$. The dimension d is assumed to be $d \geq 2$.

In this background, we again apply the covariant holographic entanglement entropy (11) to our non-static spacetime (7). The extremal surface γ_A can be specified by

$$x^+ = x^+(r), \quad x^- = x^-(r). \quad (30)$$

The area functional looks like

$$\text{Area} = 2R^{d-1} V_{d-2} \int_{\epsilon}^{r^*} \frac{dr}{r^{d-1}} \sqrt{1 - 2(\partial_r x^+)(\partial_r x^-) + Qr^d (\partial_r x^+)^2}, \quad (31)$$

where ϵ is the UV cut off as before.

The equation of motion leads to

$$\begin{aligned} \frac{r^{d-1}}{A} &= \frac{Qr^d (\partial_r x^+) - \partial_r x^-}{\sqrt{1 - 2(\partial_r x^+)(\partial_r x^-) + Qr^d (\partial_r x^+)^2}}, \\ \frac{r^{d-1}}{AB} &= \frac{\partial_r x^+}{\sqrt{1 - 2(\partial_r x^+)(\partial_r x^-) + Qr^d (\partial_r x^+)^2}}, \end{aligned} \quad (32)$$

where A and B are integration constants and we assume $A > 0$ and $B > 0$.

This leads to

$$\begin{aligned} \partial_r x^+ &= \frac{1}{\sqrt{\frac{A^2 B^2}{r^{2(d-1)}} + Qr^d - 2B}}, \\ \partial_r x^- &= \frac{Qr^d - B}{\sqrt{\frac{A^2 B^2}{r^{2(d-1)}} + Qr^d - 2B}}. \end{aligned} \quad (33)$$

The turning point $r = r_*$ of the extremal surface is determined by

$$\frac{A^2 B^2}{r_*^{2(d-1)}} + Q r_*^d - 2B = 0. \quad (34)$$

In this way, we obtain the relations

$$\begin{aligned} \frac{\Delta x^+}{2} &= \int_0^{r_*} \frac{dr}{\sqrt{\frac{A^2 B^2}{r^{2(d-1)}} + Q r^d - 2B}}, \\ \frac{\Delta x^-}{2} &= \int_0^{r_*} \frac{(Q r^d - B) dr}{\sqrt{\frac{A^2 B^2}{r^{2(d-1)}} + Q r^d - 2B}}. \end{aligned} \quad (35)$$

In order to take the subsystem A to be space-like, we can assume $\Delta x^+ > 0$ and $\Delta x^- < 0$.

Finally, the area of the extremal surface is computed as

$$\text{Area} = 2R^{d-1} V_{d-2} \int_\epsilon^{r_*} \frac{dr}{r^{d-1}} \cdot \frac{AB}{\sqrt{A^2 B^2 - 2B r^{2(d-1)} + Q r^{3d-2}}}. \quad (36)$$

4.1 Exact Analysis in $d = 2$

In the $d = 2$ case, we can analytically perform the previous integrations. This corresponds to a particular limit of the result discussed in [4].

We obtain

$$\begin{aligned} \Delta x^+ &= \frac{1}{\sqrt{Q}} \log \frac{1 + A\sqrt{Q}}{\sqrt{1 - QA^2}}, \\ \Delta x^- &= -AB. \end{aligned} \quad (37)$$

This can be solved into

$$A = \frac{\tanh(\sqrt{Q}\Delta x_+)}{\sqrt{Q}}. \quad (38)$$

The length is given by

$$\begin{aligned} \text{Length} &= R \log \frac{4}{\epsilon^2} + R \log \left| \frac{w_*}{2 - \frac{2w_*}{A^2 B^2}} \right| \\ &= R \log \frac{2}{\epsilon^2} + R \log \left[\frac{-\Delta^- \sinh(\sqrt{Q}\Delta x^+)}{\sqrt{Q}} \right]. \end{aligned} \quad (39)$$

Finally, the holographic entanglement entropy is found to be

$$S_A = \frac{c}{6} \log \left[\frac{-2\Delta^- \sinh(\sqrt{Q}\Delta x^+)}{\epsilon^2 \sqrt{Q}} \right]. \quad (40)$$

We can confirm that this agrees with the result in CFTs by taking the chiral limit of the analysis in [4].

It may be interesting to define the light-like limit (i.e. the limit the subsystem A gets closer to light-like) by

$$\Delta x^- \Delta x^+ = -\epsilon^2, \quad \Delta x^+ = \text{finite} > 0. \quad (41)$$

In this limit, S_A becomes finite:

$$\frac{6S_A}{c} = \frac{\text{Length}}{R} = \log \frac{2 \sinh(\sqrt{Q} \Delta x^+)}{\sqrt{Q} \Delta x^+} \simeq \log 2 + \frac{Q}{6} (\Delta x^+)^2 + O(Q^2). \quad (42)$$

4.2 The analysis in $d \geq 3$

Let us move on to the higher dimensional case. We concentrate on the case where the subsystem A is on a fixed time slice ($t = \text{fixed}$) and thus we require

$$\Delta x^+ = -\Delta x^- = \frac{l}{\sqrt{2}}, \quad (43)$$

where l is the width of the subsystem A .

Assume that the width l is very large. The length l gets infinitely large only when the denominator $\frac{A^2 B^2}{r^{2(d-1)}} + Q r^d - 2B$ develops a double zero at $r = r_*$. This condition and (34) can be solved at this degenerate point as follows

$$\begin{aligned} B &= \frac{3d-2}{4(d-1)} Q r_*^d, \\ A^2 &= \frac{8(d-1)d}{(3d-2)^2} \cdot \frac{r_*^{d-2}}{Q}. \end{aligned} \quad (44)$$

However, if we plug this in the integral we find that Δx^- gets *positively* divergent. This means that in the limit $\Delta x^+ \rightarrow +\infty$, we always find $\Delta x^- \rightarrow \infty$ and therefore the subsystem A gets time-like, which is not what we want. Thus this tells us that there exists an upper bound for l , which scales like $Q^{-1/d}$ for this connected extremal surface. Note also that we need to take $B > 1$ to satisfy (43). We find that the width is vanishing at $B = 1$.

Actually there is another candidate of the extremal surface. This is the disconnected surface simply given by $x^\pm = \text{const}$. We plotted areas as functions of the width $l/\sqrt{2} \equiv \Delta x^+ = -\Delta x^-$ in Fig.2, where we subtracted the disconnected surface area from the connected one. The covariant holographic entanglement entropy is defined by choosing the one with the minimal area among extremal surfaces as in (11). Thus our results in Fig.2 show that there is a sort of phase transition at the width $l_c \sim 2.4$ for $d = 3$ and $l_c \sim 1.2$ for $d = 4$. For $l < l_c$ the connected surfaces are favored, while for $l > l_c$ the disconnected ones are chosen. This behavior is a bit similar to the behavior in the confining backgrounds such as AdS solitons [37, 38]. Notice also that we can easily estimate $l_c \sim Q^{-1/d}$.

Naively, the existence of the energy flux $T_{++} \propto Q > 0$ just excites the system in a similar manner to finite temperature systems because the system is excited at the energy scale $Q^{1/d}$. Indeed, this speculation is true in the $d = 2$ case as can be seen from (40). However in higher dimensions $d \geq 3$, as we found here, the result of holographic entanglement entropy is rather different from that in the finite temperature system, which has a positive and extensive (finite) contribution to S_A . Our results for $d \geq 3$, plotted in Fig.2, show that there are positive contributions, but they are not extensive at all. The presence of the phase transition is a special feature of case B, which does not appear in the case A.

It might be useful to note that in the $d = 2$ case, the metric (7) is equivalent to that of the extremal rotating BTZ black hole via a coordinate transformation. However, this is not true in higher dimensions. Therefore only $d = 2$ has non-zero (thermal) entropy and it is very natural that we find the extensive behavior in this case. On the other hand, for $d \geq 3$, things are different and the systems are far from thermal states.

4.3 An Interpretation of the different results between Case A and Case B

It is clear that the difference between the case A and case B comes from the direction of energy current relative to the strip direction (see Fig.1). When the energy flows along the strip (case A), the energy does not leak from the strip. Therefore, the system gets simply excited and the entanglement entropy increases monotonically with l (see also [6] for the related argument in static systems). This intuitive expectation agrees with our result of HEE in section 3.

However, in case B, the strip extends in the direction orthogonal to the energy flow and thus there is a constant energy exchange with adjacent regions. In this non-trivial setup, our holographic analysis shows that there is a maximal width $l_c \sim Q^{1/d}$ above which S_A gets constant.

Since the system we consider have the energy flux $T_{++} \sim Q$, each excited mode has the wave length of order $(T_{++})^{1/d} \sim Q^{1/d}$, which is analogous to the thermal screening length at finite temperature. Thus for a larger subsystem $l > l_c$, there is no correlation⁴ or entanglement between the deep inside of A and B except the regions near the boundary of A . This explains why S_A in the case B does not depend on l when $l > l_c$. As usual, the large N limit amplifies this phenomena and leads to the sharp phase transition. On the other hand, if we consider the correlation in the direction orthogonal to the energy current as in case A, then there is no screening effect and thus there is no phase transition.

⁴ Indeed, in the replica method, the calculation of entanglement entropy can be regarded as the correlation function of two defects which produce the deficit angles. In two dimensional CFTs, they are reduced to two point functions of twisted vertex operators [39]. We can also generalize this into higher dimensions in principle [34, 40].

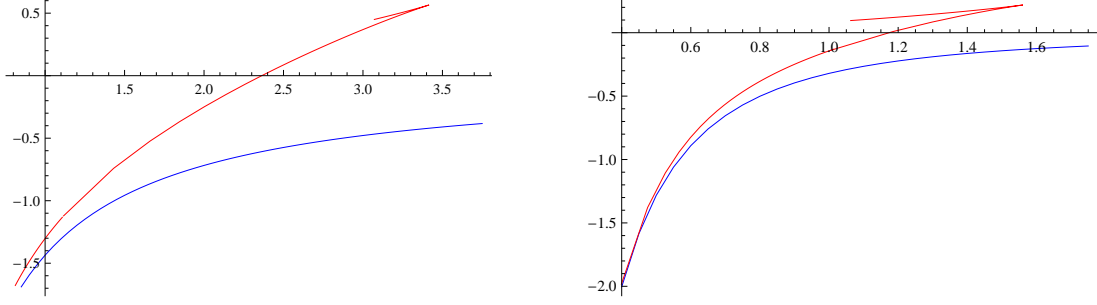


Figure 2: Numerical plots of the regularized areas of extremal surfaces as functions of the width $l = \sqrt{2}\Delta x^+ = -\sqrt{2}\Delta x^-$ of A . We set $Q = R = 1$. The left and right graph corresponds to the results for $d = 3$ and $d = 4$, respectively. In each graph, the blue curve corresponds to the connected surface in the pure AdS space while the red one to the connected one in the AdS plane wave. The area is regularized by subtracting the area of the disconnected surface given by $x^\pm = \text{constant}$.

4.4 Regularized AdS plane wave: x^\pm -coordinates

To understand better the phase transition above, let us regulate the AdS plane wave with the non-extremal background (4) containing a horizon at r_0 : for concreteness, we consider regulating the AdS_5 plane wave in terms of the boosted black D3-brane and Case B, with the strip width parallel to x_3 . Then the entanglement entropy is given by

$$S_A \sim V_2 \int \frac{dr}{r^3} \sqrt{\frac{1}{1-r_0^4 r^4} - 2(\partial_r x^+)(\partial_r x^-) + Qr^4 \left(\partial_r x^+ + \frac{r_0^4}{2Q} \partial_r x^- \right)^2}. \quad (45)$$

The conserved momenta give

$$\begin{aligned} \frac{r^3}{A} &= \frac{Qr^4 \left(\partial_r x^+ + \frac{r_0^4}{2Q} \partial_r x^- \right) - \partial_r x^-}{\sqrt{\frac{1}{1-r_0^4 r^4} - 2(\partial_r x^+)(\partial_r x^-) + Qr^4 \left(\partial_r x^+ + \frac{r_0^4}{2Q} \partial_r x^- \right)^2}}, \\ \frac{r^3}{AB} &= \frac{\partial_r x^+ - \frac{r_0^4 r^4}{2} \left(\partial_r x^+ + \frac{r_0^4}{2Q} \partial_r x^- \right)}{\sqrt{\frac{1}{1-r_0^4 r^4} - 2(\partial_r x^+)(\partial_r x^-) + Qr^4 \left(\partial_r x^+ + \frac{r_0^4}{2Q} \partial_r x^- \right)^2}}, \end{aligned} \quad (46)$$

This gives

$$\begin{aligned} \partial_r x^- &= \frac{Qr^4 - B + \frac{Br_0^4 r^4}{2}}{1 - r_0^4 r^4} \frac{1}{\sqrt{\frac{A^2 B^2}{r^6} (1 - r_0^4 r^4) + Qr^4 \left(1 + \frac{r_0^4}{2Q} B \right)^2 - 2B}}, \\ \partial_r x^+ &= \frac{1 - \frac{r_0^4 r^4}{2} - \frac{Br_0^8 r^4}{4Q}}{1 - r_0^4 r^4} \frac{1}{\sqrt{\frac{A^2 B^2}{r^6} (1 - r_0^4 r^4) + Qr^4 \left(1 + \frac{r_0^4}{2Q} B \right)^2 - 2B}}. \end{aligned} \quad (47)$$

Then we have

$$\begin{aligned}\Delta x^- &= \int_0^{r^*} dr \frac{Qr^4 - B + \frac{Br_0^4 r^4}{2}}{1 - r_0^4 r^4} \frac{1}{\sqrt{\frac{A^2 B^2}{r^6} (1 - r_0^4 r^4) + Qr^4 (1 + \frac{r_0^4}{2Q} B)^2 - 2B}}, \\ \Delta x^+ &= \int_0^{r^*} dr \frac{1 - \frac{r_0^4 r^4}{2} - \frac{Br_0^8 r^4}{4Q}}{1 - r_0^4 r^4} \frac{1}{\sqrt{\frac{A^2 B^2}{r^6} (1 - r_0^4 r^4) + Qr^4 (1 + \frac{r_0^4}{2Q} B)^2 - 2B}}.\end{aligned}\quad (48)$$

The entanglement entropy finally becomes

$$S_A \sim V_2 \int_\epsilon^{r^*} \frac{dr}{r^3} \frac{AB}{\sqrt{A^2 B^2 - A^2 B^2 r_0^4 r^4 - 2B r^6 + (1 + \frac{r_0^4}{2Q} B)^2 Q r^{10}}}\quad (49)$$

For $r_0 = 0$ and $Q = 0$, these expressions reduce to those for AdS_5 . In the limit $r_0 \rightarrow 0$ with Q fixed, these expressions can be seen to reduce to (35) (36) for the AdS_5 plane wave.

For the unboosted black brane $Q = \frac{r_0^4}{2}$ with x^\pm appearing symmetrically, we can set $B = 1$: this then gives $\partial_r x^- = \frac{-r^3}{\sqrt{(A^2 - 2r^6)(1 - r_0^4 r^4)}} = -\partial_r x^+$, $S_A \sim V_2 \int_0^{r^*} \frac{dr}{r^3} \frac{A}{\sqrt{(A^2 - 2r^6)(1 - r_0^4 r^4)}}$, giving $\partial_r t = \frac{1}{\sqrt{2}}(\partial_r x^+ + \partial_r x^-) = 0$ and the expected bulk minimal surface on a constant time slice. The denominator in these expressions is a factorized limit of those in (47), (48), (49).

More generally, let us consider the boosted black brane with $\lambda^2 = \frac{2Q}{r_0^4} \neq 1$: the AdS plane wave arises in the extreme limit of infinite boost $\lambda \rightarrow \infty$. Then it can be seen that the denominator in (47), (48), (49), can always be factorized as in the unboosted case above if $B = \frac{2Q}{r_0^4} = \lambda^2$. At this factorization point, we have $\Delta x^- = \int_0^{r^*} dr \frac{(-2Q/r_0^4)}{\sqrt{(\frac{A^2 B^2}{r^6} - 2B)(1 - r_0^4 r^4)}}$, $\Delta x^+ = \int_0^{r^*} dr \frac{1}{\sqrt{(\frac{A^2 B^2}{r^6} - 2B)(1 - r_0^4 r^4)}}$, with $S_A \sim V_2 \int \frac{dr}{r^3} \frac{AB}{\sqrt{(A^2 B^2 - 2B r^6)(1 - r_0^4 r^4)}}$. This gives $\Delta x^- = -\lambda^2 \Delta x^+$, *i.e.* $\sqrt{2} \Delta t = \lambda \Delta x^+ + \lambda^{-1} \Delta x^- = 0$. Furthermore, we have $\sqrt{2} \lambda \partial_r t = \partial_r x^- + \lambda^2 \partial_r x^+ \propto (-B + \frac{2Q}{r_0^4}) = 0$, *i.e.* we have a constant- t bulk minimal surface. Here $t = \frac{\lambda x^+ + \lambda^{-1} x^-}{\sqrt{2}}$ is the unboosted time coordinate: recall that the $[x^\pm \leftrightarrow (t, x_3)]$ -coordinate-transformation maps the boosted AdS black brane (3) to an unboosted brane. Thus the factorization point $B = \frac{2Q}{r_0^4}$ is simply the case where $\partial_r t = 0$ for the extremal surface, *i.e.* the surface is at constant- t . This is of course the usual connected constant-time extremal surface in the AdS black brane corresponding to the unboosted observer, rewritten in x^\pm -coordinates (with the momentum B tuned as above). From the point of view of the boosted brane, this is not the most natural: $T = \frac{x^+ + x^-}{\sqrt{2}}$ is the more natural time coordinate for the boosted case.

With a view to obtaining large values for Δx^\pm *i.e.* large size, we note that the parameters A, B can be tuned to a location where there is a double zero of the denominator surface, giving

$\Delta x^\pm \rightarrow \infty$: this happens when

$$\begin{aligned} V(r_*) &\equiv A^2 B^2 - A^2 B^2 r_0^4 r_*^4 - 2B r_*^6 + \left(1 + \frac{r_0^4}{2Q} B\right)^2 Q r_*^{10} = 0, \\ V'(r_*) &= -2A^2 B^2 r_0^4 r_*^3 - 6B r_*^5 + 5\left(1 + \frac{r_0^4}{2Q} B\right)^2 Q r_*^9 = 0. \end{aligned} \quad (50)$$

A rough plot of this surface $V(r)$ suggests that the nature of the surface does not change much for small r_0 . In particular, we can expand these expressions in powers of r_0^4 to obtain the leading corrections

$$B = \frac{5}{6} Q r_*^4 + \frac{17}{36} Q r_0^4 r_*^8 + \dots, \quad A^2 = \frac{24}{25} \frac{r_*^2}{Q} + \frac{4}{125} \frac{r_0^4 r_*^6}{Q} + \dots. \quad (51)$$

So it appears that the double zero location shifts a little from the AdS_5 plane wave values (44) but continues to exist with small r_0 -dependent corrections: Δx^\pm are positively divergent. This is perhaps not surprising since the scale $Q^{1/4}$ governing the AdS plane wave is widely separated from the horizon scale r_0 in the near-extremal limit with small r_0 .

More generally, eliminating the parameter A in (50), we obtain

$$A^2 B^2 = \frac{(2B r_*^6 - (1 + \frac{r_0^4}{2Q} B)^2 Q r_*^{10})}{1 - r_0^4 r_*^4}, \quad (52)$$

and a quadratic equation for B which is solved as

$$B_- = \left(\frac{2Q}{r_0^4}\right) \frac{6 - 7r_0^4 r_*^4 + 3r_0^8 r_*^8 - 2\sqrt{3}(1 - r_0^4 r_*^4)\sqrt{3 - r_0^4 r_*^4}}{r_0^4 r_*^4 (5 - 3r_0^4 r_*^4)}. \quad (53)$$

Expanding about $r_0^4 r_*^4 \sim 0$, we see that this root matches the AdS plane wave values with the leading r_0 -corrections (51), while the other root B_+ diverges in the AdS plane wave limit ($r_0 \rightarrow 0$) and is discarded. This admits a real solution and thus the double zero location exists only if the discriminant is positive, *i.e.*

$$r_*^4 \leq \frac{3}{r_0^4}. \quad (54)$$

Note that this location is inside the horizon at $r_0^4 r^4 = 1$.

One might have worried that the phase transition we observed is an artifact due to the singularity at the IR limit $r \rightarrow \infty$. Regulating the AdS plane wave geometry by placing an event horizon in the IR, we have calculated the holographic entanglement entropy (HEE) to see if there is any problem. This regularized AdS plane wave is obtained by boosting the AdS Schwarzschild black brane: the x^\pm -coordinates appear in some ways inconvenient computationally from the point of view of identifying the connected bulk extremal surface for large subsystem size as appropriate for the boosted observer. Instead it turns out to be more convenient to use different coordinates as we will describe below: we will later map this to the present discussion.

4.5 Regularized AdS Plane Wave: other coordinates

Consider the HEE in the regularized AdS plane wave for the strip subsystem (width l) in the case B. This is equivalent to the HEE in the AdS Schwarzschild black hole

$$ds^2 = \frac{dr^2}{r^2(1-r_0^4 r^4)} - \frac{1-r_0^4 r^4}{r^2} dt^2 + \frac{dy^2 + \sum_{i=1}^{d-2} dx_i^2}{r^2}, \quad (55)$$

for the strip subsystem defined by the interval $(\Delta X^+, \Delta X^-)$. They are related by

$$Q = \frac{r_0^4 \lambda^2}{2}, \quad \Delta X^+ = \frac{\lambda l}{\sqrt{2}}, \quad \Delta X^- = -\frac{l}{\sqrt{2} \lambda}, \quad (56)$$

where $X^\pm = \frac{t \pm y}{\sqrt{2}}$. Below we focus on the $d = 4$ case.

By solving the equations for the extremal surface γ_A as before, in the end we find that the size of the strip is given by

$$\Delta y = 2 \int_\epsilon^{r_*} dr \frac{r^3}{\sqrt{(a^2 b^2 - r^6)(1 - r_0^4 r^4) + b^2 r^6}}, \quad (57)$$

$$\Delta t = 2 \int_\epsilon^{r_*} dr \frac{-b r^3}{(1 - r_0^4 r^4) \sqrt{(a^2 b^2 - r^6)(1 - r_0^4 r^4) + b^2 r^6}}, \quad (58)$$

where r_* is defined by

$$(a^2 b^2 - r_*^6)(1 - r_0^4 r_*^4) + b^2 r_*^6 = 0. \quad (59)$$

The area of γ_A is written as

$$\text{Area} = 2 \int_\epsilon^{r_*} \frac{dr}{r^3} \cdot \frac{ab}{\sqrt{(a^2 b^2 - r^6)(1 - r_0^4 r^4) + b^2 r^6}}. \quad (60)$$

In order to keep the inside of the square root i.e. the function

$$g(r) = (a^2 b^2 - r^6)(1 - r_0^4 r^4) + b^2 r^6, \quad (61)$$

positive, we need to require

$$|b| < \frac{\sqrt{3}(1 - r_0^4 r_*^4)}{\sqrt{3 - r_0^4 r_*^4}}, \quad (62)$$

which is equivalent to $g'(r_*) < 0$. For simplicity, we will set $r_0 = 1$ without losing the generality. If we define $r = r_*$ to be the turning point, we have $g(r_*) = 0$ and therefore we find

$$a^2 b^2 = \frac{r_*^6(1 - r_*^4) - r_*^6 b^2}{1 - r_*^4} (\geq 0). \quad (63)$$

In this regularized geometry, there is no disconnected solution as it cannot penetrate the horizon. This guarantees completely well-controlled calculations. Then we need to ask if we can smoothly take the limit $\lambda \rightarrow \infty$, where the horizon is pushed into the deep IR and the AdS plan wave is

recovered. To see this, it is crucial to check if we can realize the extremal surface γ_A corresponds to any arbitrary large values of Δy and Δt with the space-like condition $|\Delta y| > |\Delta t|$.

Thus let us study the limits where Δy and Δt get divergent. They are given by some combinations of (i) the limit $r_* \rightarrow 1$, where γ_A approaches to the horizon, and (ii) the condition where $g(r)$ develops the double zero. Thus first we define an infinitesimally small parameter by $\eta = 1 - r_* > 0$. The double zero condition is equivalent to the condition $g'(r_*) = 0$ and this fixes b in terms of r_* as follows:

$$b = \frac{\sqrt{3}(1 - r_*^4)}{\sqrt{3 - r_*^4}} \simeq 2\sqrt{6}\eta + O(\eta^2). \quad (64)$$

Therefore we can take the second infinitesimally small parameter ϵ to be

$$\epsilon = -b + \frac{\sqrt{3}(1 - r_*^4)}{\sqrt{3 - r_*^4}} \simeq -b + 2\sqrt{6}\eta. \quad (65)$$

So we have *two* infinitesimally small positive parameters $\eta > 0$ and $\epsilon > 0$ which control the limits.

Now we define the near horizon coordinate by

$$\delta = r_* - r. \quad (66)$$

Then we can expand $g(r)$ near the turning point $r = r_*$ as follows

$$\begin{aligned} g(r) &= c_1\epsilon\delta + c_2\delta^2 + O(\delta^3), \\ c_1 &= 4\sqrt{6} + O(\eta) + O(\epsilon), \\ c_2 &= 24 + O(\eta) + O(\epsilon). \end{aligned} \quad (67)$$

It is also useful to note

$$1 - r^4 = 4\delta + 4\eta + O(\eta^2). \quad (68)$$

We can estimate (57) and (58) by using the above approximation. This leads to

$$\begin{aligned} \Delta y &\sim 2 \int_0^1 d\delta \frac{1}{\sqrt{c_1\epsilon\delta + c_2\delta^2}} = -\frac{4}{\sqrt{c_2}} \cdot \log \left[\frac{\sqrt{c_1c_2\epsilon}}{c_2 + \sqrt{c_2(c_2 + c_1\epsilon)}} \right], \\ \Delta t &\sim -2b \int_0^1 d\delta \frac{1}{4(\delta + \eta)\sqrt{c_1\epsilon\delta + c_2\delta^2}} = -\frac{(2\sqrt{6}\eta - \epsilon)}{\sqrt{\eta(c_2\eta - c_1\epsilon)}} \cdot \operatorname{arctanh} \left[\frac{\sqrt{c_2\eta - c_1\epsilon}}{\sqrt{\eta(c_2 + c_1\epsilon)}} \right]. \end{aligned} \quad (69)$$

Notice that since $b \geq 0$, we need to require

$$2\sqrt{6}\eta - \epsilon \geq 0. \quad (70)$$

We can think of many different limits, where both ϵ and η go to zero. It is always true that Δy gets divergent as

$$\Delta y \simeq -\frac{1}{\sqrt{6}} \log \epsilon. \quad (71)$$

Now we take the following limit

$$\epsilon \sim \eta^k \rightarrow 0, \quad (72)$$

with $k \geq 1$. This leads to the divergent Δt as follows

$$\Delta t \simeq \frac{1}{2} \log \frac{\epsilon}{\eta} \simeq \frac{k-1}{2k} \log \epsilon, \quad (73)$$

where we have employed the expansion: $\operatorname{arctanh}(1-x) \simeq -\frac{1}{2} \log(x/2) + O(x)$ in the limit $x \rightarrow 0$.

Thus we find

$$\frac{|\Delta t|}{|\Delta y|} = \frac{\sqrt{6}}{2} \cdot \frac{k-1}{k}. \quad (74)$$

This shows that we can construct a connected extremal surface which leads to $\Delta y \rightarrow \infty$ (i.e. infinitely large width) for any ratio which satisfies

$$0 < \frac{|\Delta t|}{|\Delta y|} < \frac{\sqrt{6}}{2}. \quad (75)$$

This covers all regions we wanted. In this way, we can conclude that the AdS plane wave limit $\lambda \rightarrow \infty$ is smooth.

To compare with our previous discussions in the x^\pm -coordinates, we can map the coefficients A, B in (49) and a, b in (60): this gives

$$b = \frac{1 - \frac{B}{\lambda^2}}{1 + \frac{B}{\lambda^2}}, \quad (76)$$

and correspondingly for the parameter a . The double zero location B_- in (53) then maps to

$$b = \frac{1 - \frac{B}{\lambda^2}}{1 + \frac{B}{\lambda^2}} = \frac{\sqrt{3}(1 - r_0^4 r_t^4)}{\sqrt{3 - r_0^4 r_t^4}}, \quad (77)$$

in agreement with (59), (62). This then recasts (48) as

$$\begin{aligned} \Delta x^- &= \int \frac{\lambda^2 \left(\frac{r_0^4 r^4}{2} \left(1 + \frac{B}{\lambda^2} \right) - \frac{B}{\lambda^2} \right)}{(1 - r_0^4 r^4) \sqrt{\dots}} = \int \frac{\lambda^2 (b - (1 - r_0^4 r^4)) dr}{(1+b)(1 - r_0^4 r_t^4) \sqrt{\frac{a^2 b^2}{r^6} (1 - r_0^4 r^4) - (1 - b^2) + r_0^4 r^4}}, \\ \Delta x^+ &= \int \frac{1 - \frac{r_0^4 r^4}{2} \left(1 + \frac{B}{\lambda^2} \right)}{(1 - r_0^4 r^4) \sqrt{\dots}} = \int \frac{(b + (1 - r_0^4 r^4)) dr}{(1+b)(1 - r_0^4 r_t^4) \sqrt{\frac{a^2 b^2}{r^6} (1 - r_0^4 r^4) - (1 - b^2) + r_0^4 r^4}}. \end{aligned} \quad (78)$$

We then have

$$\Delta x^- = -\frac{\lambda^2}{1+b} (\Delta t + \Delta y), \quad \Delta x^+ = -\frac{1}{1+b} (\Delta t - \Delta y). \quad (79)$$

A constant t surface has $\Delta x^- = -\lambda^2 \Delta x^+$, as expected. Scaling to the double zero $b \rightarrow 0$, and to the horizon $r_0 r_* \rightarrow 1$, with b scaling faster as in (72), we see that Δx^\pm acquire log-divergences $\Delta x^+ \rightarrow k_1 \log(\dots)$, $\Delta x^- \rightarrow -k_2 \lambda^2 \log(\dots)$, corresponding to a spacelike surface as long as the constants k_1, k_2 are not identical. The AdS plane wave calculation can be defined as the limit $r_0 \rightarrow 0$, $r_* \rightarrow \infty$, $r_0 r_* \rightarrow 1$ with the scaling above: this is effectively equivalent to the disconnected surface mentioned earlier. Thus the overall picture of the extremal surfaces appears consistent.

5 Conclusions

AdS plane waves arise as normalizable null deformations of $AdS \times S$ spaces [7, 9]: they are dual to excited CFT states with lightcone momentum density T_{++} turned on. These spacetimes are likely α' -exact string backgrounds similar to plane waves and $AdS_5 \times S^5$. With $T_{++} \sim Q$ uniform, these spacetimes are spatially homogenous and can be obtained as certain limits of boosted AdS Schwarzschild black branes [8]. Thus they are among the simplest anisotropic and excited systems in holographic setups. The AdS_5 plane wave upon x^+ -dimensional reduction gives a background lying in the hyperscaling violating family with “ $\theta = d - 1$ ”, exhibiting logarithmic behavior of entanglement entropy holographically. In the higher dimensional description, the corresponding extremal surface lies on a constant lightcone time x^- slice and extends along the x^+ -direction.

In this paper, we have explored holographic entanglement entropy (HEE) for these AdS_{d+1} plane waves for strip-shaped (spacelike) subsystems. There are two different cases: case A and case B as explained in Fig.1. In both case, the leading divergent contribution to HEE is the familiar area law term. The finite part behaves differently in the two cases.

When the strip is parallel to the energy flux (case A), the finite part of HEE is a monotonically increasing function of the width l of the strip. Though it is smaller than the extensive thermal entropy, it is always greater than the HEE for the pure AdS dual to the ground state. In the AdS_5 plane wave case, this finite piece grows logarithmically as $S_A^{finite} \sim V_2 \sqrt{Q} \log(lQ^{1/4})$ with size l and is perhaps a finite reflection of the log-growth in the null case above. It was argued in [23, 24] that hyperscaling violating metrics with “ $\theta = d - 1$ ” are dual to systems with Fermi surfaces. Indeed, if we regard $Q^{1/4}$ as the scale of fermi momentum (energy) k_F , then S_A^{finite} agrees with the expected behavior in systems with fermi surfaces [23]. It is therefore interesting to obtain a deeper understanding of the origin of the logarithmic behavior in the AdS_5 plane wave backgrounds from a field theory point of view. In particular, one would like to understand if this behaviour is due to a Fermi surface or some alternative mechanism. In the AdS_4 plane wave case, the finite part grows with l like $S_A^{finite} \sim V_1 \sqrt{l} \sqrt{Q}$, so that the logarithmic term in the AdS_5 case is replaced by the power, \sqrt{l} . To the best of our knowledge, the AdS_4 plane wave is the first known example of a construction arising from string theory which gives rise to such a power law enhancement.

On the other hand, when the strip is orthogonal to the energy flux (case B), we find a phase transition such that for l larger than $l_c \sim Q^{-1/d}$, the HEE becomes constant. Using the regulated description in terms of boosted AdS Schwarzschild black branes with horizon at r_0 , we have seen that this behaviour persists for small r_0 : this is expected since the scale Q is more dominant here. For general boost, the connected extremal surface can be identified in a certain scaling limit where the surface approaches the horizon (and develops a double zero).

One possible intuitive explanation of these different behaviors in case A and case B is as follows. Since the system we consider has the energy flux $T_{++} \sim Q$, each excited mode has the wave length of order $(T_{++})^{1/d} \sim Q^{1/d}$ along the energy flux direction. Therefore in case B, where the HEE measures the correlation in the flux direction, the HEE gets trivial (i.e. constant) for a large width $l > l_c \sim Q^{1/d}$ because we can regard l_c as the correlation length. This is the reason why we found the phase transition phenomenon in our holographic analysis of case B. On the contrary, in the direction orthogonal to the flux, the situation is similar to the ground state and the correlation length should be infinite. Therefore we do not have any phase transition in case A. It is very interesting to analyze the same question from CFT calculations in e.g. free field theories.

Acknowledgements: TT thanks I. Klebanov, A. Lawrence, S. Ryu for useful discussions. We thank the Organizers of the String Theory Discussion Meeting, June '12, at the International Center for Theoretical Sciences (ICTS), Bangalore, where this work began. KN and SPT thank the Organizers of the Indian Strings Meeting (ISM2012), Puri, India for hospitality at the final stages of this work. TT is grateful to the organizers and to the Princeton Center for Theoretical Science for the workshop “Entanglement in Discrete and Continuous Quantum Systems,” where the result of this work was presented. SPT would like to acknowledge the hospitality of the Yukawa Institute Of Theoretical Physics during his visit to attend the workshop on ”Gauge/Gravity Duality” where some of this research was done. KN is partially supported by a Ramanujan Fellowship, Department of Science and Technology, Govt of India. TT is supported by JSPS Grant-in-Aid for Challenging Exploratory Research No.24654057. TT is partially supported by World Premier International Research Center Initiative (WPI Initiative) from the Japan Ministry of Education, Culture, Sports, Science and Technology (MEXT). SPT acknowledges support from the J. C. Bose Fellowship, Department of Science and Technology, Govt of India.

References

- [1] P. Calabrese and J. Cardy, “Entanglement entropy and conformal field theory,” *J. Phys. A* **42** (2009) 504005 [arXiv:0905.4013 [cond-mat.stat-mech]].
- [2] T. Nishioka, S. Ryu and T. Takayanagi, “Holographic Entanglement Entropy: An Overview,” *J. Phys. A* **42** (2009) 504008; T. Takayanagi, “Entanglement Entropy from a Holographic Viewpoint,” *Class. Quant. Grav.* **29** (2012) 153001 [arXiv:1204.2450 [gr-qc]].
- [3] P. Calabrese and J. Cardy, “Evolution of entanglement entropy in one-dimensional systems,” *J. Stat. Mech.* **0504**, P04010 (2005) [arXiv:cond-mat/0503393].
- [4] V. E. Hubeny, M. Rangamani and T. Takayanagi, “A Covariant holographic entanglement entropy proposal,” *JHEP* **0707** (2007) 062 [arXiv:0705.0016 [hep-th]].
- [5] J. Abajo-Arrestia, J. Aparicio and E. Lopez, “Holographic Evolution of Entanglement Entropy,” *JHEP* **1011** (2010) 149 [arXiv:1006.4090 [hep-th]]; T. Albash and C. V. Johnson, “Evo-

- lution of Holographic Entanglement Entropy after Thermal and Electromagnetic Quenches,” *New J. Phys.* **13** (2011) 045017 [arXiv:1008.3027 [hep-th]]; V. Balasubramanian, A. Bernamonti, J. de Boer, N. Copland, B. Craps, E. Keski-Vakkuri, B. Muller and A. Schafer *et al.*, “Thermalization of Strongly Coupled Field Theories,” *Phys. Rev. Lett.* **106** (2011) 191601 [arXiv:1012.4753 [hep-th]].
- [6] J. Bhattacharya, M. Nozaki, T. Takayanagi and T. Ugajin, “Thermodynamical Property of Entanglement Entropy for Excited States,” arXiv:1212.1164 [hep-th].
- [7] K. Narayan, “On Lifshitz scaling and hyperscaling violation in string theory,” *Phys. Rev. D* **85** (2012) 106006 [arXiv:1202.5935 [hep-th]].
- [8] H. Singh, “Lifshitz/Schrödinger Dp-branes and dynamical exponents,” *JHEP* **1207** (2012) 082 [arXiv:1202.6533 [hep-th]]; H. Singh, “Special limits and non-relativistic solutions,” *JHEP* **1012**, 061 (2010) [arXiv:1009.0651 [hep-th]].
- [9] K. Narayan, “AdS null deformations with inhomogeneities,” *Phys. Rev. D* **86**, 126004 (2012) [arXiv:1209.4348 [hep-th]].
- [10] R. A. Janik and R. B. Peschanski, “Asymptotic perfect fluid dynamics as a consequence of AdS/CFT,” *Phys. Rev. D* **73**, 045013 (2006) [hep-th/0512162].
- [11] D. Grumiller and P. Romatschke, “On the collision of two shock waves in AdS(5),” *JHEP* **0808**, 027 (2008) [arXiv:0803.3226 [hep-th]].
- [12] G. T. Horowitz and N. Itzhaki, “Black holes, shock waves, and causality in the AdS / CFT correspondence,” *JHEP* **9902**, 010 (1999) [hep-th/9901012]; R. Emparan, “Exact gravitational shock waves and Planckian scattering on branes,” *Phys. Rev. D* **64**, 024025 (2001) [hep-th/0104009]; G. Arcioni, S. de Haro and M. O’Loughlin, “Boundary description of Planckian scattering in curved space-times,” *JHEP* **0107**, 035 (2001) [hep-th/0104039].
- [13] K. Goldstein, S. Kachru, S. Prakash, S. P. Trivedi, “Holography of Charged Dilaton Black Holes,” *JHEP* **1008**, 078 (2010) [arXiv:0911.3586 [hep-th]]; K. Goldstein, N. Iizuka, S. Kachru, S. Prakash, S. P. Trivedi, A. Westphal, “Holography of Dyonically Charged Dilaton Black Branes,” *JHEP* **1010**, 027 (2010) [arXiv:1007.2490 [hep-th]].
- [14] M. Cadoni, G. D’Appollonio and P. Pani, “Phase transitions between Reissner-Nordstrom and dilatonic black holes in 4D AdS spacetime,” *JHEP* **1003**, 100 (2010) [arXiv:0912.3520 [hep-th]].
- [15] C. Charmousis, B. Gouteraux, B. S. Kim, E. Kiritsis and R. Meyer, “Effective Holographic Theories for low-temperature condensed matter systems,” *JHEP* **1011**, 151 (2010) [arXiv:1005.4690 [hep-th]].
- [16] E. Perlmutter, “Domain Wall Holography for Finite Temperature Scaling Solutions,” *JHEP* **1102**, 013 (2011) [arXiv:1006.2124 [hep-th]].
- [17] B. Gouteraux and E. Kiritsis, “Generalized Holographic Quantum Criticality at Finite Density,” *JHEP* **1112**, 036 (2011) [arXiv:1107.2116 [hep-th]].
- [18] G. Bertoldi, B. A. Burrington and A. W. Peet, “Thermal behavior of charged dilatonic black branes in AdS and UV completions of Lifshitz-like geometries,” *Phys. Rev. D* **82**, 106013 (2010) [arXiv:1007.1464 [hep-th]]; G. Bertoldi, B. A. Burrington, A. W. Peet and I. G. Zadeh, “Lifshitz-like black brane thermodynamics in higher dimensions,” *Phys. Rev. D* **83**, 126006 (2011) [arXiv:1101.1980 [hep-th]].
- [19] N. Iizuka, N. Kundu, P. Narayan and S. P. Trivedi, “Holographic Fermi and Non-Fermi Liquids with Transitions in Dilaton Gravity,” *JHEP* **1201**, 094 (2012) [arXiv:1105.1162 [hep-th]].

- [20] M. Alishahiha and H. Yavartanoo, “On Holography with Hyperscaling Violation,” JHEP **1211**, 034 (2012) [arXiv:1208.6197 [hep-th]].
- [21] J. Bhattacharya, S. Cremonini and A. Sinkovics, “On the IR completion of geometries with hyperscaling violation,” arXiv:1208.1752 [hep-th].
- [22] N. Kundu, P. Narayan, N. Sircar and S. P. Trivedi, “Entangled Dilaton Dyons,” arXiv:1208.2008 [hep-th].
- [23] N. Ogawa, T. Takayanagi and T. Ugajin, “Holographic Fermi Surfaces and Entanglement Entropy,” JHEP **1201** (2012) 125 [arXiv:1111.1023 [hep-th]].
- [24] L. Huijse, S. Sachdev and B. Swingle, “Hidden Fermi surfaces in compressible states of gauge-gravity duality,” Phys. Rev. B **85** (2012) 035121 [arXiv:1112.0573 [cond-mat.str-el]].
- [25] X. Dong, S. Harrison, S. Kachru, G. Torroba and H. Wang, “Aspects of holography for theories with hyperscaling violation,” arXiv:1201.1905 [hep-th].
- [26] B. S. Kim, “Schrödinger Holography with and without Hyperscaling Violation,” JHEP **1206**, 116 (2012) [arXiv:1202.6062 [hep-th]].
- [27] P. Dey and S. Roy, “Lifshitz-like space-time from intersecting branes in string/M theory,” arXiv:1203.5381 [hep-th]; “Intersecting D-branes and Lifshitz-like space-time,” arXiv:1204.4858 [hep-th].
- [28] E. Perlmutter, “Hyperscaling violation from supergravity,” JHEP **1206**, 165 (2012) [arXiv:1205.0242 [hep-th]].
- [29] M. Ammon, M. Kaminski and A. Karch, “Hyperscaling-Violation on Probe D-Branes,” arXiv:1207.1726 [hep-th].
- [30] M. Kulaxizi, A. Parnachev and K. Schalm, “On Holographic Entanglement Entropy of Charged Matter,” JHEP **1210**, 098 (2012) [arXiv:1208.2937 [hep-th]].
- [31] J. Maldacena, D. Martelli and Y. Tachikawa, “Comments on string theory backgrounds with non-relativistic conformal symmetry,” JHEP **0810**, 072 (2008) [arXiv:0807.1100 [hep-th]].
- [32] K. Balasubramanian and K. Narayan, “Lifshitz spacetimes from AdS null and cosmological solutions,” JHEP **1008**, 014 (2010) [arXiv:1005.3291 [hep-th]]; A. Donos and J. P. Gauntlett, “Lifshitz Solutions of D=10 and D=11 supergravity,” JHEP **1012**, 002 (2010) [arXiv:1008.2062 [hep-th]]; R. Gregory, S. L. Parameswaran, G. Tasinato and I. Zavala, “Lifshitz solutions in supergravity and string theory,” JHEP **1012**, 047 (2010) [arXiv:1009.3445 [hep-th]]; D. Casiani and A. F. Faedo, “Constructing Lifshitz solutions from AdS,” arXiv:1102.5344 [hep-th]; N. Halmagyi, M. Petrini and A. Zaffaroni, “Non-Relativistic Solutions of N=2 Gauged Supergravity,” arXiv:1102.5740 [hep-th]; K. Narayan, “Lifshitz-like systems and AdS null deformations,” Phys. Rev. D **84**, 086001 (2011) [arXiv:1103.1279 [hep-th]]; W. Chemissany and J. Hartong, “From D3-Branes to Lifshitz Space-Times,” Class. Quant. Grav. **28**, 195011 (2011) [arXiv:1105.0612 [hep-th]].
- [33] K. Copley and R. Mann, “Singularities in Hyperscaling Violating Spacetimes,” arXiv:1210.1231 [hep-th].
- [34] S. Ryu and T. Takayanagi, “Holographic derivation of entanglement entropy from AdS/CFT,” Phys. Rev. Lett. **96** (2006) 181602; “Aspects of holographic entanglement entropy,” JHEP **0608** (2006) 045.
- [35] L. Bombelli, R. K. Koul, J. Lee and R. D. Sorkin, “A Quantum Source of Entropy for Black Holes,” Phys. Rev. D **34** (1986) 373; M. Srednicki, “Entropy and area,” Phys. Rev. Lett. **71** (1993) 666 [hep-th/9303048].

- [36] H. Casini and M. Huerta, “Entanglement and alpha entropies for a massive scalar field in two dimensions,” *J. Stat. Mech.***0512**:P12012,2005; H. Casini and M. Huerta, “Entanglement entropy in free quantum field theory,” *J. Phys. A* **42** (2009) 504007 [arXiv:0905.2562 [hep-th]].
- [37] T. Nishioka and T. Takayanagi, “AdS Bubbles, Entropy and Closed String Tachyons,” *JHEP* **0701** (2007) 090 [hep-th/0611035].
- [38] I. R. Klebanov, D. Kutasov and A. Murugan, “Entanglement as a probe of confinement,” *Nucl. Phys. B* **796** (2008) 274 [arXiv:0709.2140 [hep-th]].
- [39] P. Calabrese and J. Cardy, “Entanglement entropy and quantum field theory,” *J. Stat. Mech.* **0406**, P002 (2004) [arXiv:hep-th/0405152].
- [40] L. -Y. Hung, R. C. Myers, M. Smolkin and A. Yale, “Holographic Calculations of Renyi Entropy,” *JHEP* **1112** (2011) 047 [arXiv:1110.1084 [hep-th]].